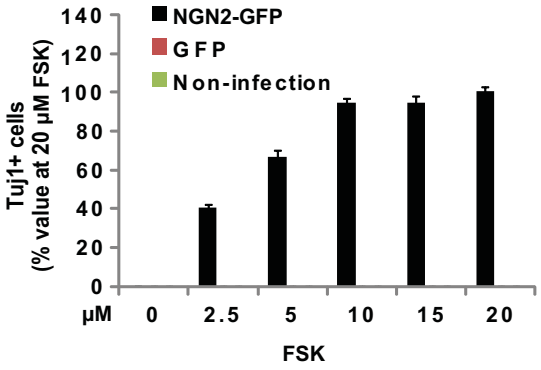

Supplementary Figure S1. Neuronal conversion in response to different dosage of forskolin (FSK). Tuj1$^+$ cells were examined 5 days post treatment of IMR-90 fibroblasts (means ± s.e.m., n=20 randomly selected 20x fields from triplicate samples). Tuj1$^+$ cells were undetectable in non-infected or control virus-infected fibroblasts under the same culture condition.

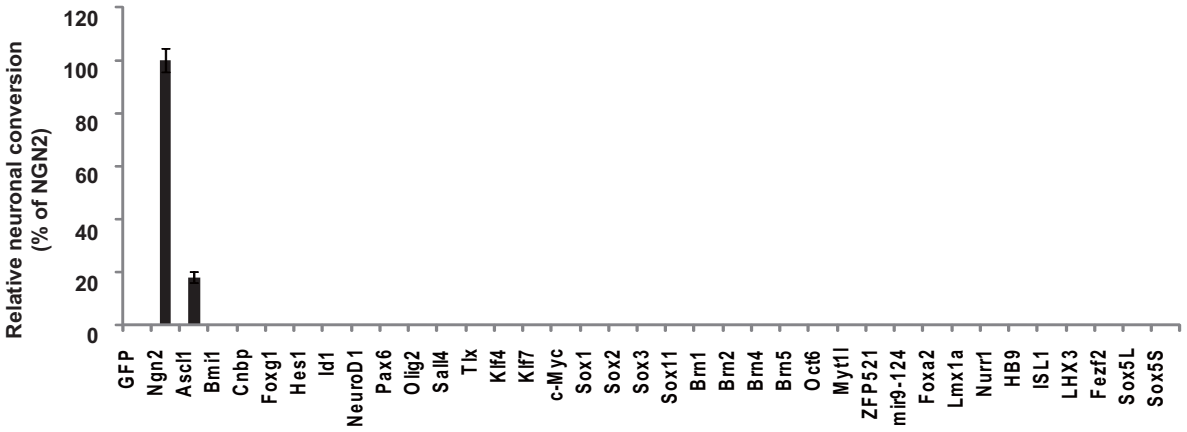

Supplementary Figure S2. FSK and DM uniquely synergize with NGN2 to reprogram human fetal fibroblasts to neurons. Tuj1^{+} cells from IMR-90 fibroblasts were quantified after 5 days of incubation with FSK and DM (means ± s.e.m., n=20 randomly selected 20x fields from triplicate samples.)

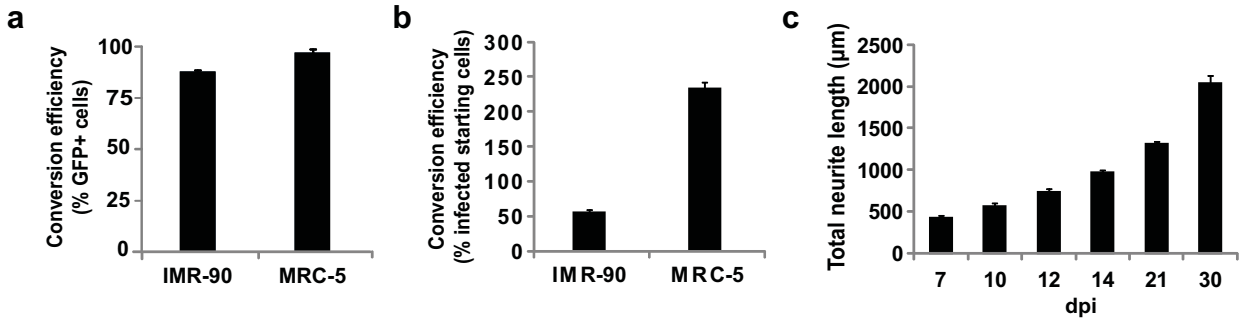

Supplementary Figure S3. Small molecule-mediated efficient conversion of human fetal fibroblasts by NGN2. (**a-b**) Conversion efficiency at 14 dpi. Total number of Tuj1^{+} cells was normalized to that of either NGN2-expressing (GFP^{+}) or infected starting cells (means ± s.e.m., n=3). (**c**) Neurite growth of converted neurons over time (means ± s.e.m., n=10 cells).

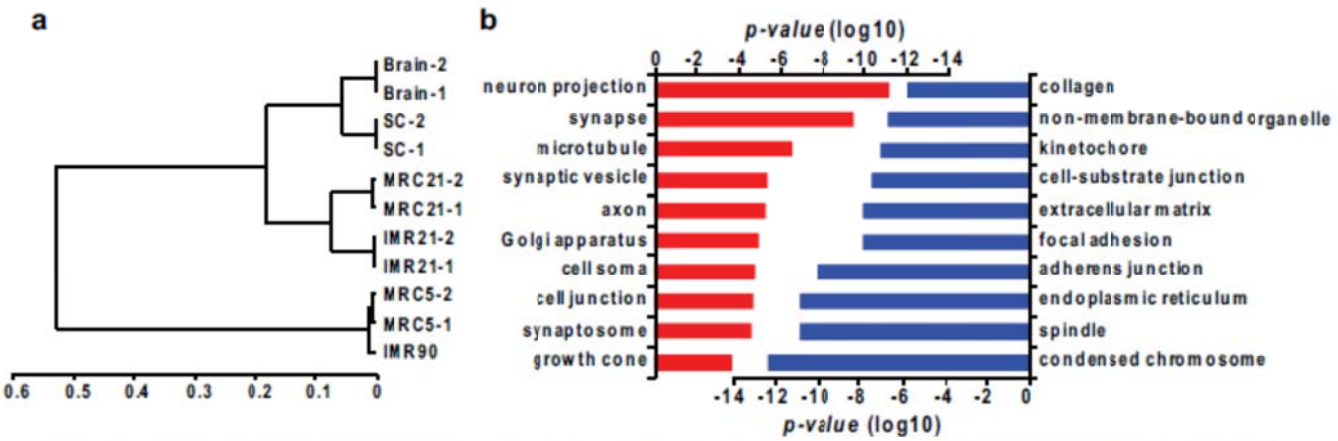

Supplementary Figure S4. Gene expression analysis of induced neurons by NGN2. (**a**) Hierarchical clustering of global gene expression. MRC21 and IMR21 represent reprogrammed cells from MRC-5 and IMR-90 fibroblasts in duplicate at 21 dpi, respectively. IMR-90 and MRC-5 are non-reprogrammed human fetal lung fibroblasts. Adult human brain and spinal cord (SC) were used as controls. (**b**) Top ten highly enriched gene sets by DAVID ontology analysis. Red and blue bars indicate significantly up-regulated and down-regulated genes, respectively.

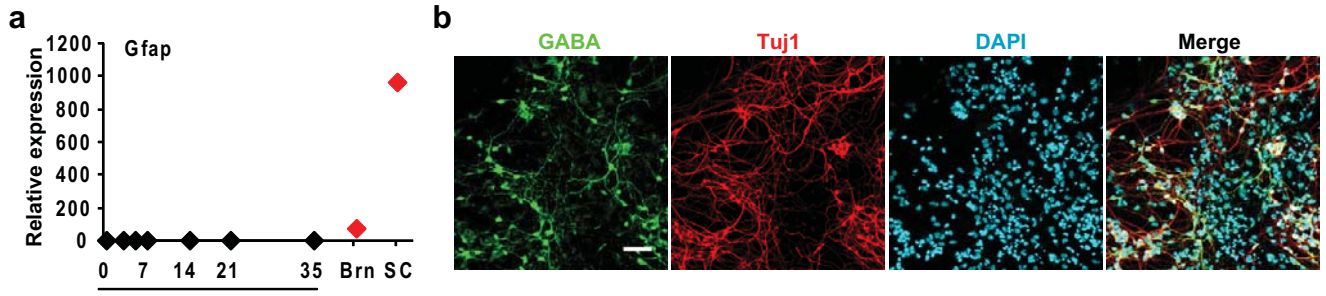

Supplementary Figure S5. Gene expression analysis of converted neurons from human fetal fibroblasts. (**a**) qRT-PCR analysis of a marker for glia during reprogramming (n=3 independent samples at the indicated time points). Samples from adult human brain (Brn) or spinal cord (SC) were used as controls (n=1). (**b**) GABA expression in neurons differentiated from human neural stem cells. This was a positive control for GABA antibody used in **Figure 1o**. Scale, 50 μm.

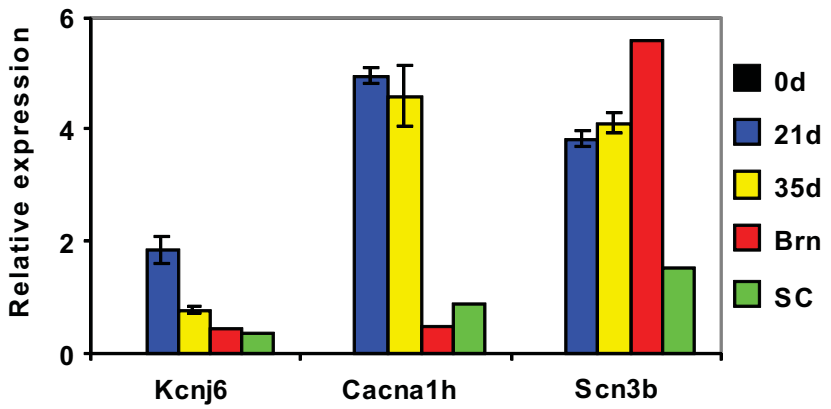

Supplementary Figure S6. Channels for potassium (Kcnj6), calcium (Cacna1h) and sodium (Scn3b) were induced in converted neurons (means ± s.e.m., n=3). Samples from adult human brain (Brn) and spinal cord (SC) were used as controls (n=1).

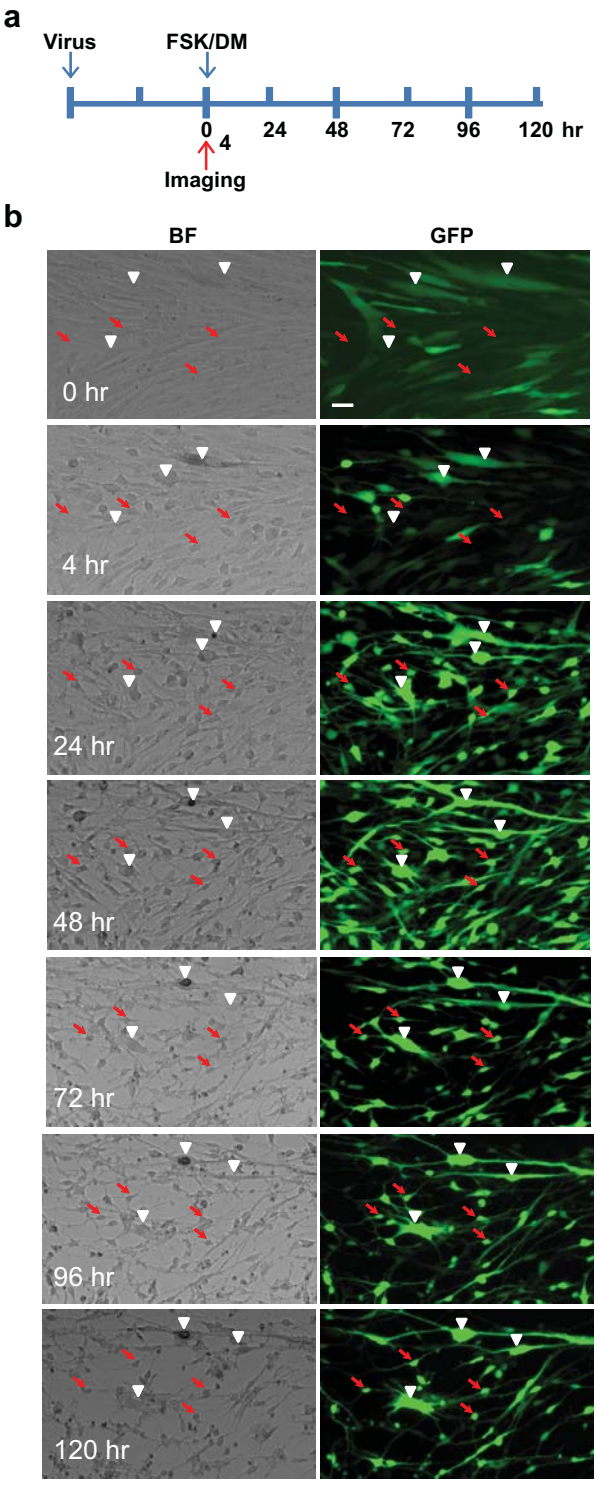

Supplementary Figure S7. Small molecules enable NGN2 to induce rapid morphological change of fibroblasts into neuron-like cells. (**a**) Experimental design. (**b**) Time-lapse live cell images taken at the indicated time points after treatment with FSK/DM. The same imaging fields are indicated by white arrowheads, whereas red arrows point to cells rapidly changing shape into neuron-like morphology without going through cell divisions. Scale, 50 μm.

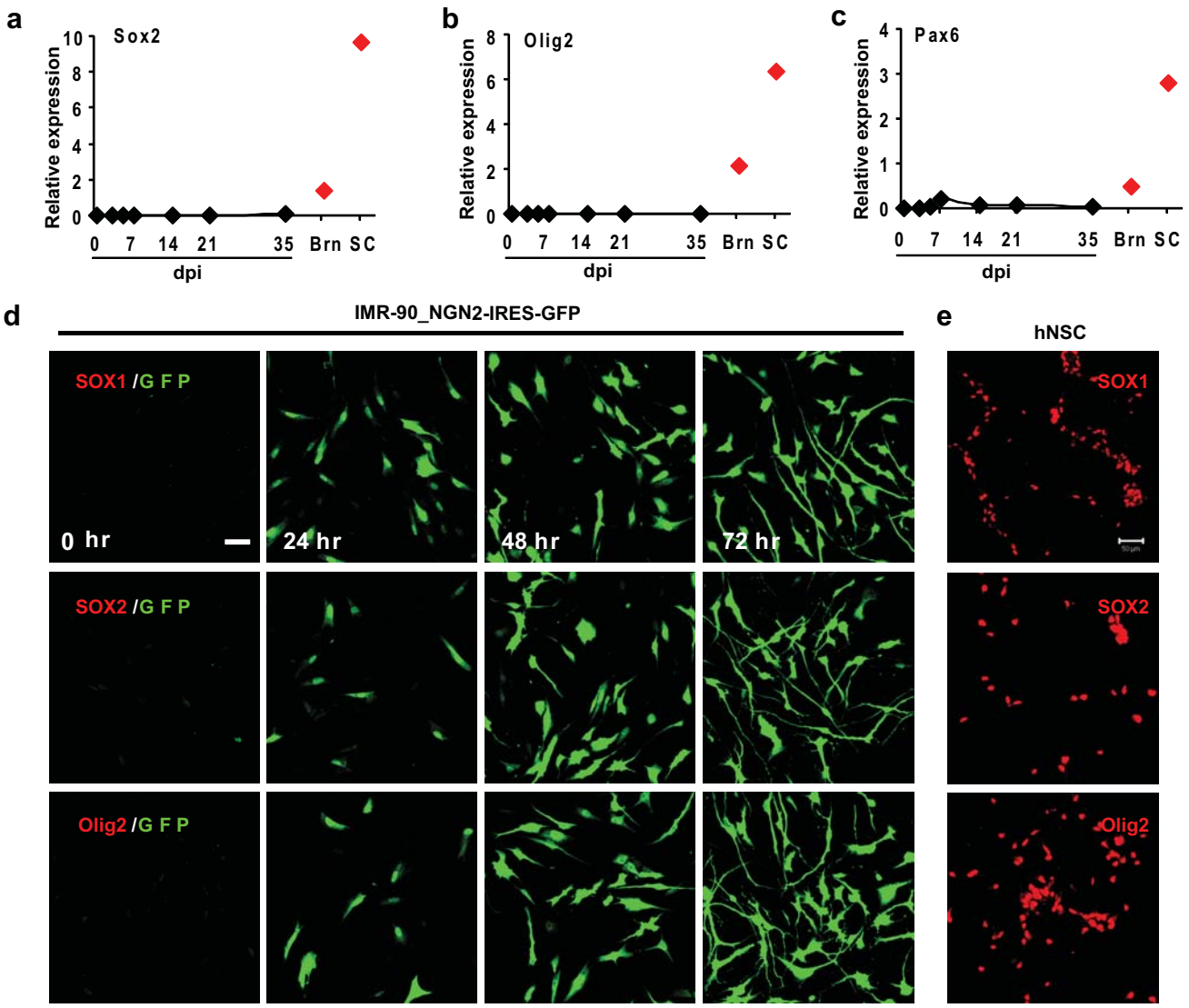

Supplementary Figure S8. Neuronal conversion from human fibroblasts does not pass through a progenitor state. (**a-c**) qRT-PCR analysis of markers for neural progenitors (means ± s.e.m., n=3 independent samples at the indicated time points). Samples from adult human brain (Brn) or spinal cord (SC) were used as controls (n=1). (**d**) Markers for neural progenitors were not detected during the reprogramming process. (**e**) Antibody specificity was examined in human neural stem cells (hNSC). Scales, 50 μm.

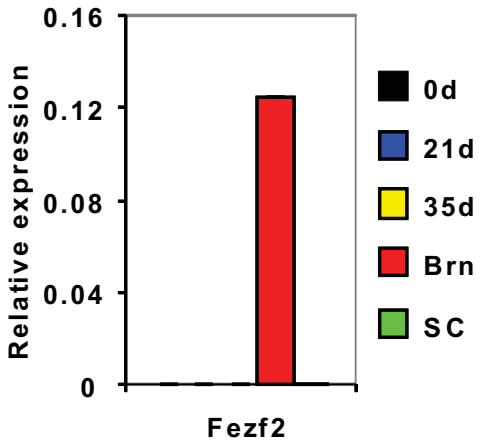

Supplementary Figure S9. Fezf2, a marker for upper motor neurons, was not detected in induced neurons by qRT-PCR (means ± s.e.m., n=3). Samples from adult human brain (Brn) and spinal cord (SC) were used as controls (n=1).

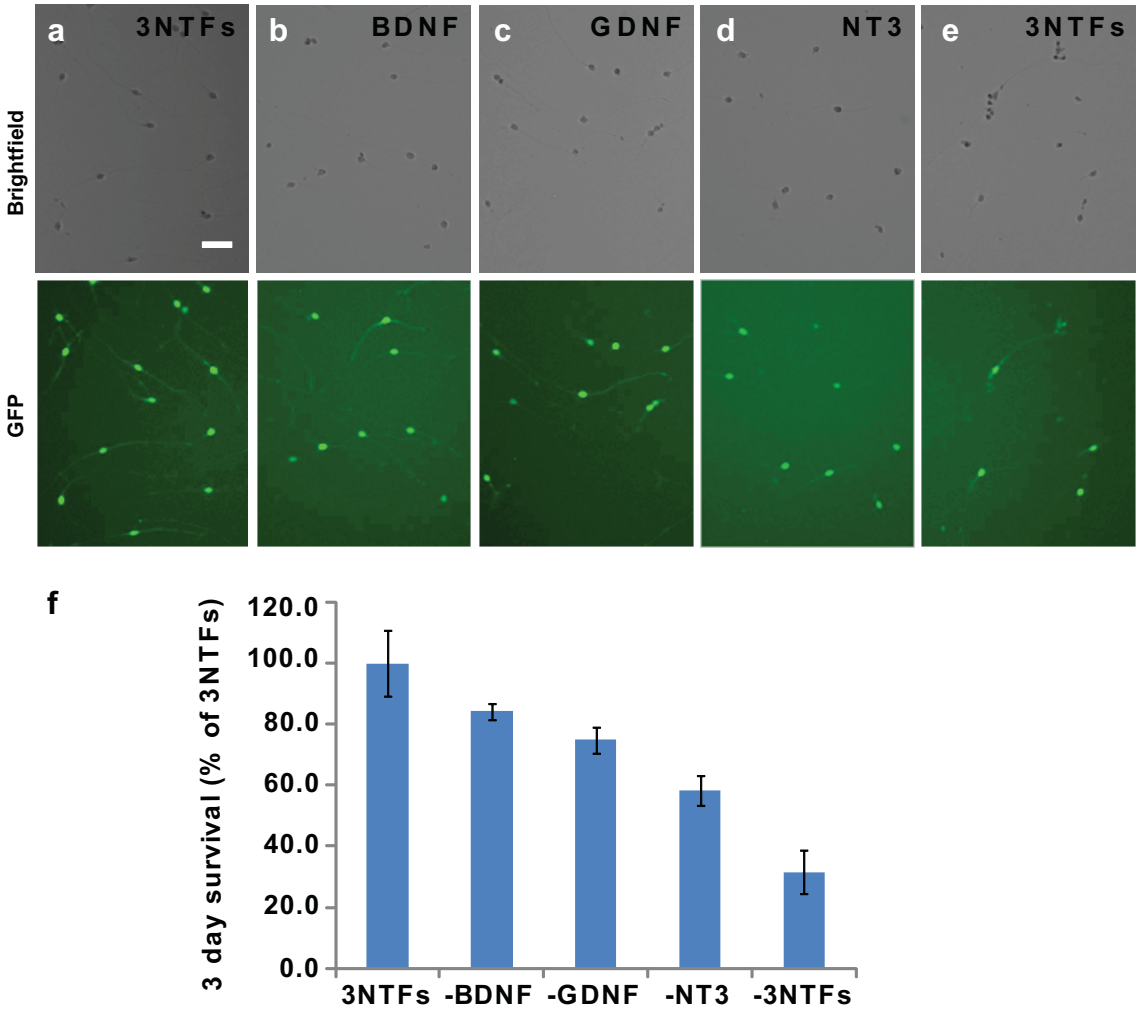

Supplementary Figure S10. NGN2-induced neurons depend on neurotrophic factors for long-term survival. (**a-f**) Withdrawing any of the indicated neurotrophic factors resulted in a loss of purified converted neurons. Surviving GFP^+ cells were counted 3 days after removal of the indicated factors from triplicate samples (means ± s.e.m.). Scale, 50 μm.

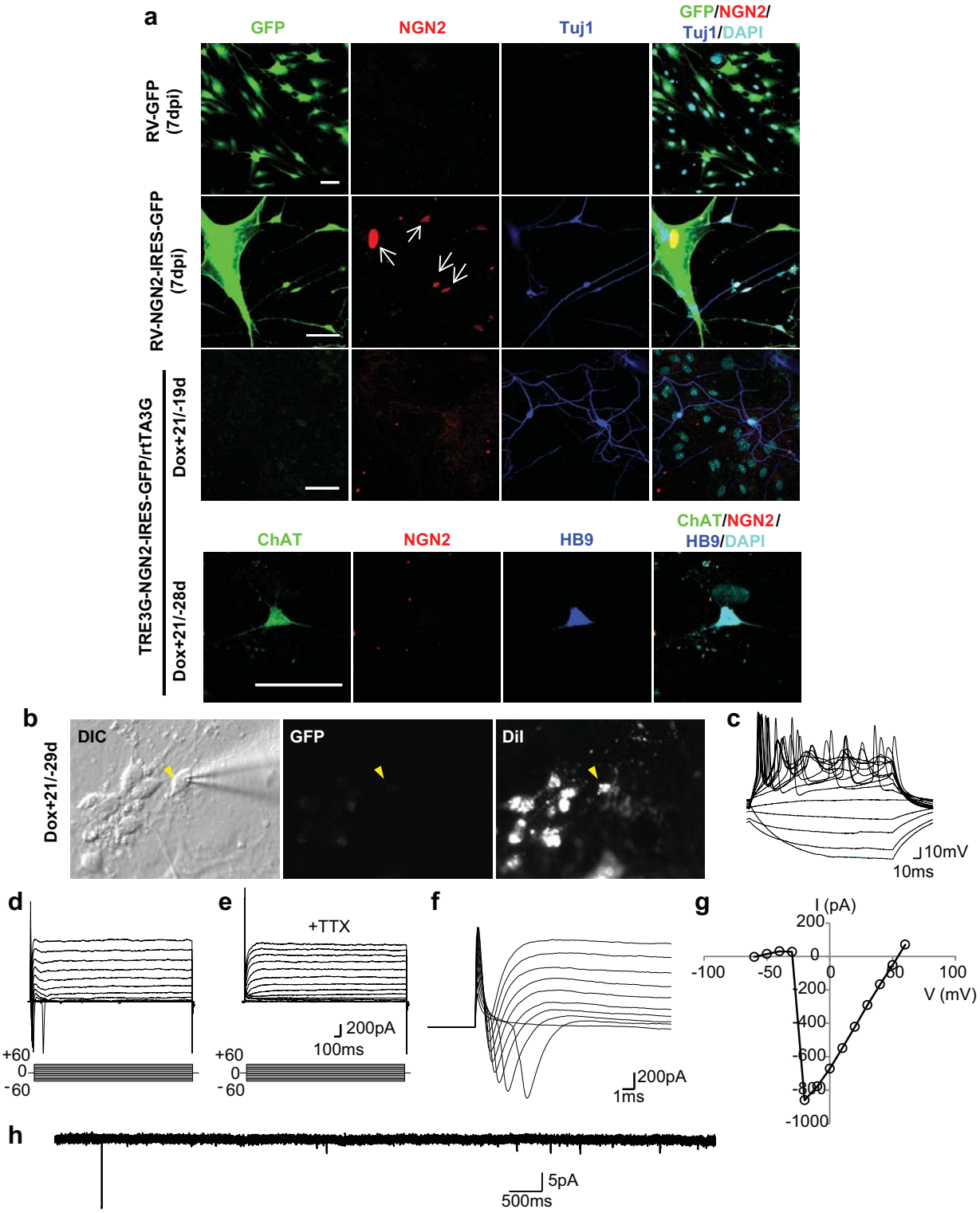

Supplementary Figure S11. Reprogrammed neurons are functionally mature after downregulation of exogenous NGN2. (**a**) Immunocytochemistry analysis showing hiCNs from MRC-5 fibroblasts express ChAT and HB9 at 49 dpi after turning off NGN2 expression by Dox withdrawal at 21 dpi (Dox+21/-28d). Lack of NGN2 expression was confirmed by staining at both 19 d and 28 d post Dox withdrawal. Antibody specificity was examined at 7 dpi using retrovirus (RV)-expressed NGN2-IRES-GFP (arrows). RV-GFP was used as a negative control. (**b**) Representative image of a patched hiCN 29 d post Dox withdrawal (Dox+21/-29d). These hiCNs were labeled at 21 dpi by DiI before plating on astrocytes-coated coverslips. (**c**) Action potentials were elicited by depolarizing current injection (-20 pA to +40 pA with 5pA interval) and resembled functionally mature neurons (n=8/8 recorded cells). (**d-e**) TTX-sensitive fast inward currents upon depolarization by voltage steps. (**f-g**) Sodium currents elicited above -30mV, with a peak current at -800 pA (n=5/7 recorded cells). (**h**) Spontaneous activity recorded from hiCNs co-cultured with mouse astrocytes (n=9/10 recorded cells). Scale, 50 μm.

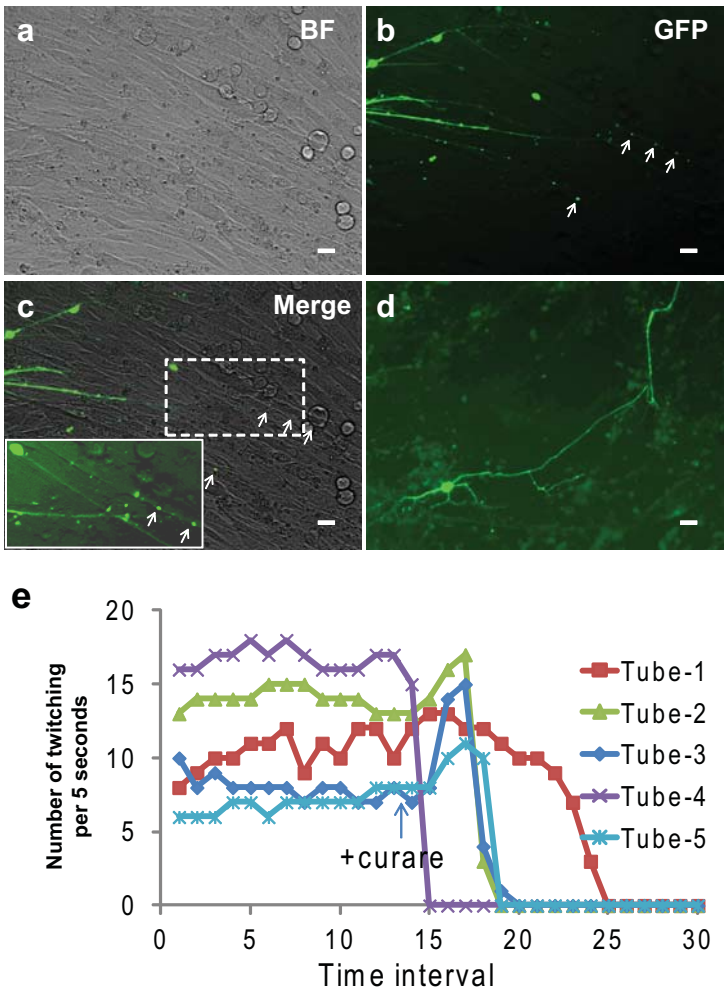

Supplementary Figure S12. hiCNs induce curare-sensitive contractions of co-cultured myotubes. (**a-c**) hiCNs extended long axons along the length of differentiated C2C12 myotubes and formed synaptic-like punctate structures (arrows). Live cell images were taken 7 days post co-culture. Scale, 50 μm. (**d**) hiCNs survived over 2 weeks in myotube-co-culture even in the absence of exogenous neurotrophic factors. (**e**) hiCNs stimulated rhythmic myotube contractions, which were sensitive to curare treatment.

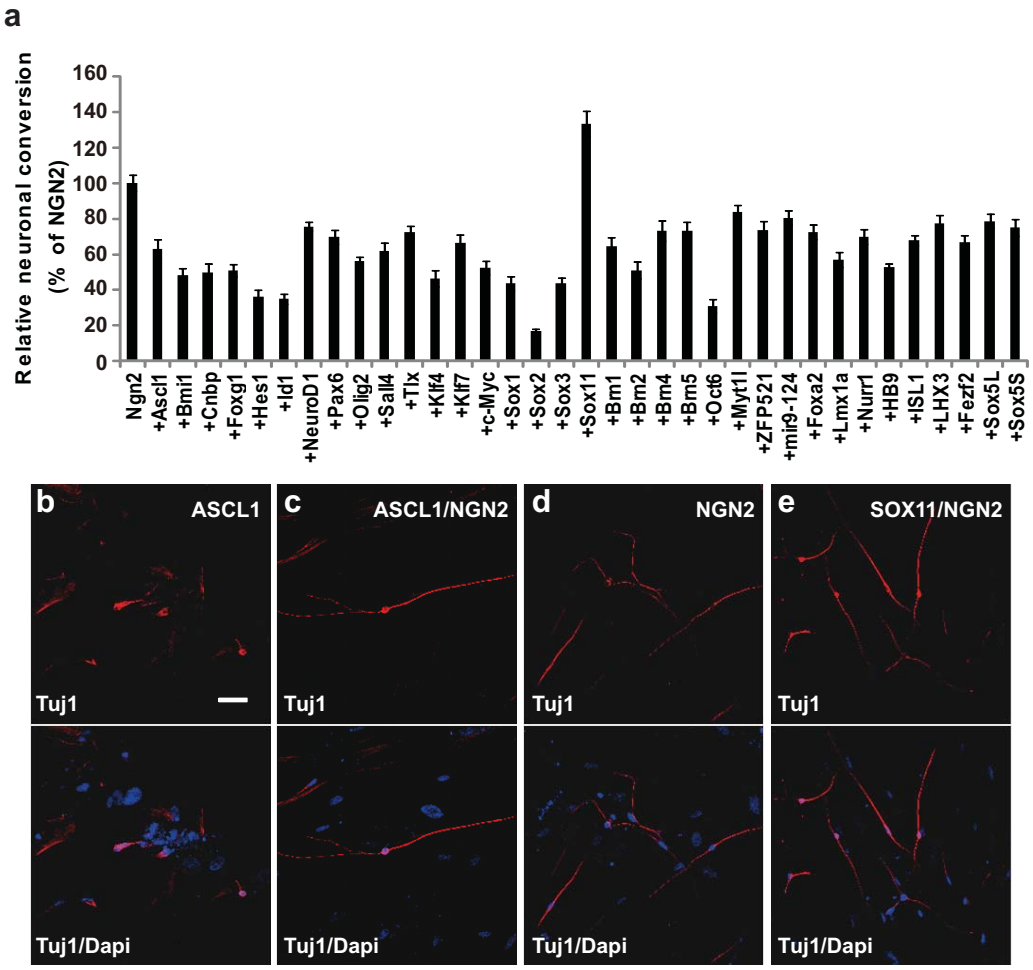

Supplementary Figure S13. Enhancing NGN2 activity by SOX11. (**a**) IMR-90 fibroblasts were transduced with virus expressing NGN2 alone or in combination with the indicated factors. Tuj1$^+$ cells were scored at 7 dpi (means ± s.e.m., n=20 randomly selected 20x fields from triplicate samples). (**b-e**) Representative images of Tuj1$^+$ cells at 7 dpi. The ASCL1-induced Tuj1$^+$ cells showed very primitive unipolar morphology. Scale, 50 μm.

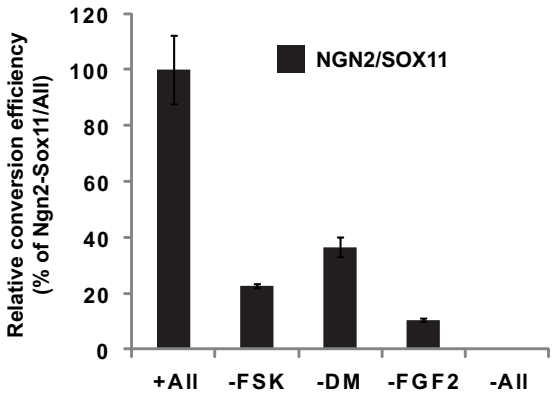

Supplementary Figure S14. Highly efficient neuronal conversion from adult fibroblasts requires each of the identified extrinsic factors. $Tuj1^+$ cells were counted at 21 dpi (means ± s.e.m., n=3 wells).

Supplementary Table S1. List of small molecules

	Name (Abbreviation)	Company (Catalog No.)	Function and Involved Signaling Pathway	Solvent (concentration)
1	Forskolin (FSK)	Sigma (F6886)	cAMP activator, PKA pathway	DMSO (10 μM)
2	Retinoic Acid (RA)	Sigma (R2625)	RA signaling pathways	DMSO (1 μM)
3	Valproic Acid (VPA)	Sigma (P4543)	HDAC inhibitor, GSK3β inhibitor, Notch-1 activator	DW (1 mM)
4	n-Butyric Acid (NaB)	Sigma (B-5887)	HDAC inhibitor	DW (1 mM)
5	Trichostatin A (TSA)	Sigma (T8552)	HDAC inhibitor	DW (0.1 μM)
6	SB431542 (SB)	Sigma (S4317)	TGF-βR Inhibitor, Activin/TGF-β/SMAD signaling pathways	DMSO (10 μM)
7	Dorsomorphin Compound C (DM)	EMD Chemicals (171260)	BMP inhibitor, BMP/SMAD signaling pathways	DMSO (1 μM)

Supplementary Table S2. List of genes examined for reprogramming human fibroblasts into neurons

	Gene Name	Gene ID
1	Ngn2	63973
2	Ascl1	429
3	Bmi1	12151
4	Cnbp	12785
5	Foxg1	2290
6	Hes1	15205
7	Id1	15901
8	NeuroD1	4760
9	Pax6	5080
10	Olig2	10215
11	Sall4	99377
12	Tlx	21907
13	Klf4	9314
14	Klf7	93691
15	c-Myc	4609
16	Sox1	20664
17	Sox2	6657
18	Sox3	20675
19	Sox11	20666
20	Brn1	18993
21	Brn2	5454
22	Brn4	5456
23	Brn5	19009
24	Oct6	18991
25	Myt1l	17933

26	ZNF521	25925
27	mir9 cluster	407046, 407047, 407051
28	mir124	406907
29	Foxa2	15376
30	Lmx1a	110648
31	Nurr1	18227
32	HB9	3110
33	ISL1	3670
34	LHX3	8022
35	Fezf2	55079
36	Sox5L	6660
37	Sox5S	6660

Supplementary Table S3. Sources of examined human fibroblasts

	Name	Repository (Catalog ID)	Origin	Age	Gender	Disease
1	IMR-90	ATCC (CCL-186)	Fetal Lung	16 Weeks Gestation	Female	Normal
2	MRC-5	ATCC (CCL-171)	Fetal Lung	14 Weeks Gestation	Male	Normal
3	GM05565	Coriell	Skin	3 Years	Male	Apparently Healthy
4	GM03813	Coriell	Skin	3 Years	Male	Spinal Muscular Atrophy
5	GM03814	Coriell	Skin	NA[a]	Female	Apparently Healthy
6	GM07522	Coriell	Skin	19 Years	Female	Apparently Healthy
7	ND29563	Coriell	Skin	37 Years	Male	Amyotrophic Lateral Sclerosis

Supplementary Table S4. qRT-PCR Primers used in this study for quantitative gene expression

Gene Name	Primer Sequences	Sense/Antisense
Cacna1h	TGACCTTCGGCAACTATGTG	Sense
	GGAGTTCTCTGAGCTTGTGG	Antisense
ChAT	GCACTCCAGCTCCTTCAC	Sense
	CACTGCACCAGGACGATG	Antisense
Fezf2	GGTACTGAAGGAAAACTCGGC	Sense
	CGGGTGAGATTATAGTGAGCG	Antisense
GFAP	GTGTCAGAAGGCCACCTCAAG	Sense
	TGGACTCCTTAATGACCTCTCCAT	Antisense
HB9	GCACCAGTTCAAGCTCAAC	Sense
	GCTGCGTTTCCATTTCATCC	Antisense
HOXA5	GCAAGCTGCACATAAGTCATG	Sense
	AGGTAACGGTTGAAGTGGAAC	Antisense
HOXA6	GTACACGAGCCCGGTTTAC	Sense
	CAGGTAGCGGTTGAAGTGG	Antisense
HOXA7	AATTTCCGCATCTACCCCTG	Sense
	GTGGGCGATTTCAATGCG	Antisense
HOXA9	AATGCTGAGAATGAGAGCGG	Sense
	GGGTCTGGTGTTTTGTATAGGG	Antisense
HOXB4	TCGTCTACCCCTGGATGC	Sense
	GTGTCAGGTAGCGGTTGTAG	Antisense
HOXB6	TGGATGCAGCGGATGAATTC	Sense
	CGTCAGGTAGCGATTGTAGTG	Antisense
HOXB7	CCTGGATGCGAAGCTCAG	Sense
	CGTCAGGTAGCGATTGTAGTG	Antisense
HOXC6	GACCAGAAAGCCAGTATCCAG	Sense
	AAATTCCTTCTCCAGTTCCAGG	Antisense
HOXC8	CTAACAGTAGCGAAGGACAAGG	Sense
	CTAGTTCCAAGGTCTGATACCG	Antisense
HOXC9	AGCACAAAGAGGAGAAGGC	Sense
	CGTCTGGTACTTGGTGTAGG	Antisense
HOXC10	AAAGGAGAGGGCCAAAGC	Sense
	GCGTCTGGTGTTTAGTATAGGG	Antisense
HOXC11	ACCGGCTGCAGTATTTCTC	Sense
	ACAGTCCAGTTTTCCACCG	Antisense
HOXD9	GGCTGTTCGCTGAAGGAG	Sense
	CGTCTGGTATTTGGTGTAGGG	Antisense
ISL2	CAACAGTATGGTGCCGAGTC	Sense
	AGAGCTTTCGGAACTGGAATG	Antisense
Kcnj6	GAACTGGAGACTGAAGAGGAAG	Sense

	GACAAGGAAAGATTGTGTTGGG	Antisense
endoNGN2	TCAGACATGGACTATTGGCAG	Sense
	GGGACAGGAAAGGGAACC	Antisense
vNGN2	TCAGACATGGACTATTGGCAG	Sense
	ACACCGGCCTTATTCCAAG	Antisense
Olig2	AGCTCCTCAAATCGCATCC	Sense
	AAAAGGTCATCGGGCTCTG	Antisense
Pax6	GCCCTCACAAACACCTACAG	Sense
	TCATAACTCCGCCCATTCAC	Antisense
Scn3b	GAAAGGTCTCAAAAGCCGAAG	Sense
	CACTGCTCCTGTTCTATTCCTC	Antisense
SMN1	CCACACCTAAAAGAAAACCTGC	Sense
	GCAATGGTAGCTGGGTAAATG	Antisense
Sox2	CCGTTCATCGACGAGGCTAA	Sense
	TAATCCGGGTGCTCCTTCAT	Antisense